RSC Advances

PAPER

Cite this: *RSC Adv.*, 2016, **6**, 51583

Application of magnesium hydroxide nanocoatings on cellulose fibers with different refining degrees

A. Sierra-Fernandez,*[ab] L. S. Gomez-Villalba,[a] M. E. Rabanal,[bc] R. Fort[a] and L. Csóka[d]

Received 21st April 2016
Accepted 17th May 2016

DOI: 10.1039/c6ra10336g

www.rsc.org/advances

Paper aging and protection are of crucial interest for improving the preservations of library collections and archives. Highly aging-resistant cellulose fiber sheets were obtained by treatment with magnesium hydroxide nanoparticles ($Mg(OH)_2$). The procedure was tested on the sheets made of bleached (B) and refined unbleached (UB) pine cellulose fibers as well as their 50%/50% mixture (M). The mor and structural properties of the obtained sheets were studied by X-ray diffraction (XRD) and Scanning Electron Microscopy (SEM) methods. Stress–strain, smoothness and pH measurements were employed to determine the changes in physical-chemical characteristics of the sheets after mixing two types of the fibers and subsequent treatment with $Mg(OH)_2$. It has been shown that the sheets made of the fiber mixture show a higher tensile index and smoothness. The modification with $Mg(OH)_2$ nanoparticles induces an increase in the pH of the sheets to slightly basic values (around pH 8), facilitates the inter-fiber bonding and additionally enhances the smoothness of the sheets. Finally, by exposing the sheets to thermo-hygrometric accelerated artificial ageing, it was found that the physical properties of the treated sheets were not significantly dependent on the environmental factors.

1. Introduction

Cellulose is one of the most abundant natural carbohydrate resources on Earth and an important raw material. It is used in the preparation of a large number of our daily-life products and materials including probably the most significant, paper, a felted sheet of cellulose fibers entangled into a dense network. The physical properties of the paper strongly depend on the fiber–fiber hydrogen bonding, network structure and drying conditions. For this reason, different strategies have been employed to modify the fiber surfaces and improve the interaction of adjacent fibers. For example, a refining process is used in the papermaking industry in order to increase the specific surface area of pulp fibers through internal and external fibrillation, fiber shortening and fines generation.[1–3] The mentioned process improves the formation of the sheets and their mechanical strength. On the other hand, due to high porosity as well as pronounced hydrophilicity, paper is prone to degradation and ageing. While biodegradation of the paper is usually treated as a good property in a recent discussions related to the waste management, it is a problem when it comes to preservations of archives and paper based cultural heritage. In order to protect and preserve the paper materials, several methods were suggested. One of them is to use alkaline-earth metal hydroxide nanoparticles such as magnesium hydroxide ($Mg(OH)_2$) that can inhibit or retard cellulose degradation. Magnesium hydroxide nanoparticles attracted lot of interests in recent years due to good thermal stability and fire retardant properties coupled with low toxicity and low cost.[4] It was also shown that the $Mg(OH)_2$ nanoparticles, typically in brucite crystal form, are excellent deacidifying agents. After their attachment to cellulose fibers, they provide an alkaline reservoir for deacidification and reduce the rate of degradation processes.[5–8] So far, the brucite $Mg(OH)_2$ nanocrystals were synthesized by using different routes, such as solvothermal,[9] sol–gel,[10] bubbling,[11] microwave-assisted,[12] and hydrothermal[13] methods. In this study, we used the hydrothermal method for the synthesis of nanocrystalline magnesium hydroxide particles, due to its simplicity, effectiveness and low-cost.[14] The brucite nanoparticles were further used for the modification of cellulose sheets in order to create protective coatings. The suggested method is in the line with our previous research studies, where Ag[15] and ZnO[16] nanoparticles were used for fabrication of the multifunctional papers with antimicrobial properties. However, in the present case, we modified with $Mg(OH)_2$ nanoparticles already prepared sheets, instead cellulose fibers. The modification procedure was tested on the sheets prepared from the unbleached and bleached fibers and their 50%/50% mixture. The aim was to investigate the influence of $Mg(OH)_2$ nanoparticles on the properties of the

[a]*Instituto de Geociencias (CSIC, UCM), C/José Antonio Novais 2, CP 28040, Madrid, Spain. E-mail: arsierra@ucm.es; a.sierra@igeo.ucm-csic.es*

[b]*University Carlos III of Madrid and IAAB, Department of Materials Science and Engineering and Chemical Engineering, Avda. Universidad 30, 28911 Leganes, Madrid, Spain*

[c]*Instituto Tecnológico de Química y Materiales Alvaro Alonso Barba (IAAB), Avda. Universidad 30, 28911 Leganés, Madrid, Spain*

[d]*University of West Hungary, Institute of Wood Based Products and Technologies, Bajcsy Zs. E. u. 4, 9400 Sopron, Hungary*

different type of cellulose sheets and to establish whether the observed effects depend on their initial morphology.

2. Experimental section

2.1. Materials and sample preparation

Cellulose fibers. Two types of pine cellulose fibers were used in this study: bleached with low lignin content (<0.5%), and non-bleached chemi-thermomechanical pulp (CTMP) with high lignin content (22.5%). Bleached pine fibers were received from Buckeye Technologies Inc. The unbleached pine fibers were collected from Dunapack Ltd, Hungary.

Synthesis of brucite ($Mg(OH)_2$) nanoparticles. Brucite nanoparticles were synthesized *via* the hydrothermal method using hydrazine hydrate ($N_2H_4 \cdot H_2O$) as a precipitant. All solvents and reagents were purchased from Sigma-Aldrich and used as received. High-purity water (18 MΩ cm^{-1}) was prepared by a deionized water purification system (Barnstead, Dubuque, IA, USA) and was used in all procedures. The procedure for the synthesis of $Mg(OH)_2$ nanoparticles is based on our recent study.[17] Briefly, 0.12 g of magnesium nitrate hexahydrate ($Mg(NO_3)_2 \times 6H_2O$) and 0.08 mL of hydrazine hydrate ($N_2H_4 \times H_2O$) were dissolved in high-purity water (15 mL) under vigorous magnetic stirring at room temperature. Stirring was continued until the white uniform suspension appeared. The mixture was transferred into a Teflon-lined stainless steel autoclave, sealed and hydrothermally treated at a constant reaction temperature of 180 °C for 12 hours. After that, the mixture was left to cool down to room temperature and washed several times using water and ethanol. Finally, the product was dried in an inert gas atmosphere at 60 °C for 7 hours to avoid $Mg(OH)_2$ carbonation. For application on the cellulose sheets, the nanoparticles were dispersed in ethanol by vigorous stirring followed by ultrasound treatment for 15 minutes. The concentration of the nanoparticles in the dispersion was 2.0 g L^{-1}.

Preparation of hand sheets. HAAGE D-4330 laboratory sheet former was used for the fabrication of the different hand sheets according to standard DIN EN ISO 5269-2. The handsheets had a basic weight of 95 g m^{-2}. Prior to sheet making the cellulose fibers were disintegrated in a laboratory pulp disintegrator machine. The sheets are also made of the 50%/50% mixture of the fibers. The initial tests in our laboratory showed that more compact sheets were obtained if the bleached fibers were refined before mixing with unbleached fibers. For this reason, the low lignin content fibers were additionally beaten (refined) up to 35 Schopper-Riegler degrees (SR°) using a commercial laboratory valley-beater. The list of samples together with treatment procedures for each type of fibers are given in Table 1.

Treatment of cellulose fiber sheets with magnesium hydroxide nanoparticles. The application of $Mg(OH)_2$ nanoparticles on the sheets was carried out by using two methods most commonly used in the conservation of documentary: spraying and immersion. Six sheets were sprayed with 2.5 mL of the $Mg(OH)_2$ nanoparticles dispersion on one side only. Another six paper sheets were immersed in the dispersion for 40 minutes. After that, they were first dried between blotting paper in order to eliminate the excess solvent and then left to dry in air at 23 °C and 50% RH for 10 days. Control samples were not subjected to any treatment. The particular methods used for the modification of the samples were also listed in Table 1. The procedure for preparation of the sheets and their modification is schematically shown in Fig. 1.

Table 1 Overview of sample sheets, preparation conditions and lignin content

Sample ID[a,b]	Pre-treatments	$Mg(OH)_2$ NPs treatment	Paper thickness (μm)
UB	Disintegration	Control	189 ± 5
UB-MH-S	Disintegration	Spraying	195 ± 5
UB-MH-I	Disintegration	Immersion	191 ± 4
B	Disintegration/refining	Control	124 ± 2
B-MH-S	Disintegration/refining	Spraying	127 ± 5
B-MH-I	Disintegration/refining	Immersion	125 ± 5
M	Mixture of UB and B	Control	110 ± 3
M-MH-S	Mixture of UB and B	Spraying	113 ± 5
M-MH-I	Mixture of UB and B	Immersion	112 ± 5

[a] UB – unbleached fibers; B – bleached fibers; M – 50%/50% mixture of UB and B fibers; MH – magnesium hydroxide. [b] S – treated by spraying method; I – treated by immersion.

Accelerated aging of cellulose samples. In order to test their aging resistance, untreated and $Mg(OH)_2$ treated cellulose fiber sheets were subjected to artificial ageing. The samples were kept for three weeks at a constant temperature of 80 °C and relative humidity of 65% in a climatic chamber (Model 700, Challenge Angelantoni Industrie). The samples were hung in the climatic chamber without touching each other or the inner walls. In addition, on each aperture of the chamber for removing the particular sheets, the remaining ones were repositioned in order to provide as uniform as possible ageing conditions.

3. Analytical methods

3.1. Morphological and chemical characterization of $Mg(OH)_2$ nanoparticles

To characterize phase purity and crystallographic structures of the magnesium hydroxide nanoparticles, XRD measurements were carried out using an X-ray diffractometer (Philips X'Pert) with Cu Kα radiation ($\lambda = 1.54$ Å). The voltage and current were set to 40 kV and 40 mA, respectively. The samples were mounted on a circular holder, and the spectra were recorded in the range of $2\theta = 10–50°$ at a scanning test of 2° min^{-1}. The average crystallite size of the magnesium hydroxide nanoparticles in the cellulose samples was estimated by Scherrer's formula, $D = K\lambda/\beta \cos\theta$, where λ is the wavelength of the X-ray radiation (in Å), K is a constant taken as 0.9, β the full width at half-maximum height (FWHM) and θ is the diffraction angle (in rad) (Khorsand Zak *et al.* 2012). The morphological study of the $Mg(OH)_2$ nanoparticles were conducted by scanning electron microscopy (SEM) (Philips XL 30/EDS D × 4) and transmission electron microscopy (TEM, JEOL JEM 2100 at 200 kV). X-ray energy dispersive spectroscopy (EDS) analyses were carried out to study the composition of the $Mg(OH)_2$ nanoparticles. The samples for

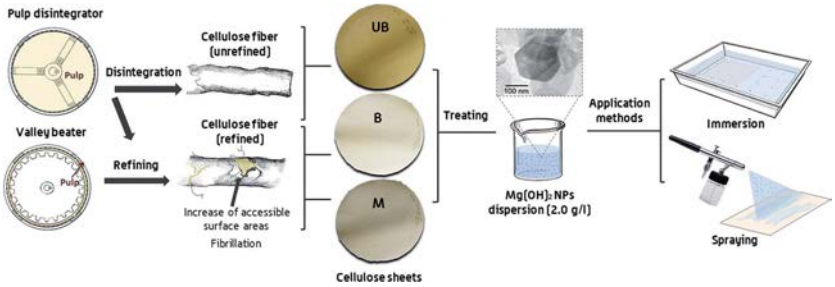

Fig. 1 A schematic illustration of the application of the magnesium hydroxide nanoparticles on the surface of unbleached (UB), bleached (B), and 50%/50% mixture of UB and B fibers (M).

TEM studies were ultrasonically dispersed in acetone and then deposited on holey carbon copper grids.

3.2. Characterization of cellulose sheets

X-ray diffraction (XRD). The crystallographic structures of the different cellulose samples were also analysed by the X-ray diffraction (XRD) (Philips X'Pert) operating under the same conditions as above. The crystallinity index (CrI) was calculated from XRD data using the Segal method[18] $\mathrm{CrI} = [(I_{002} - I_{\mathrm{am}})/I_{002}] \times 100$, where I_{002} is the maximum intensity of the (002) lattice diffraction peak (positioned at $2\theta = 22.5^{\circ}$), and I_{am} is the minimum in peak intensity between the main and secondary peaks (between the 101/10−1 and 002 lattice planes). Despite the Segal method typically yields higher CrI values than other methods, it remains optimal to comparing relative differences between cellulose samples (Park *et al.* 2010).

Scanning electron microscopy (SEM). Scanning electron microscopy (SEM) of untreated and treated fibers was carried out using a HITACHI S-3400 N instrument at an operating voltage of 17 kV. SEM images were obtained with the surface of the samples coated with a gold thin layer to avoid charging effect.

Smoothness. The smoothness of the untreated and treated cellulose fiber sheets were carried out on a Bendtsen smoothness tester. The smoothness was determined by measuring the air flow between the cellulose samples (backed by flat glass on the bottom side) and two pressurized, concentric lands that are impressed into the sample from the top side. The rate of air flow (mL min^{-1}) is related to the smoothness of the paper.

Tensile-strength. The mechanical properties of the unaged, aged, untreated and treated cellulose samples were measured in accordance with the EN ISO 1924-2 standard. The tensile tests were carried out on a universal testing machine (INSTRON 3345, USA Tensile Tester). The cross head speed was 50 mm min^{-1} and the distance between the clamps was 180 mm. The cellulose samples were rectangular in shape with a size width of 15 mm. At least three test strips of each cellulose sample were evaluated, and all the presented data were the average of these tests.

pH measurements. Prior to pH measurements, 120 mg of the samples were preconditioned at 23 °C and 50% RH for two days. Then, the samples were weighed, cut in pieces and placed inside screw top vials. 10 mL of ultrapure water (with a resistivity of 18 MΩ cm^{-1}) were added and vial was sealed. The vials were kept in ultrasound bath for 1 hour and the pH measurements of the cold water extracts were carried out with a digital pH meter (LovibondSensoDirect pH 110 model).

4. Results and discussion

4.1. Magnesium hydroxide nanoparticles

The morphology and microstructure of the $Mg(OH)_2$ nanoparticles were analysed by SEM and TEM. Fig. 2 show the SEM and TEM micrographs of $Mg(OH)_2$ particles. Both micrographs depict well-defined hexagonal nanoplates of magnesium hydroxide, with a uniform particle size of 160 ± 40 nm and a thickness of ~18 nm. The inset of Fig. 2b shows the EDAX spectra of the particles. Mg and O elements were detected in the sample with no impurities. After analysing several areas of the sample, a high chemical homogeneity and purity of the $Mg(OH)_2$ was confirmed. The EDAX peaks associated with the presence of copper (Cu) were assigned to the holey copper grid and should be ignored.

In addition, the crystal phases and crystallinity of the nanosized $Mg(OH)_2$ obtained were determined by X-ray diffraction. Fig. 3 shows the X-ray diffraction (XRD) pattern of the as-

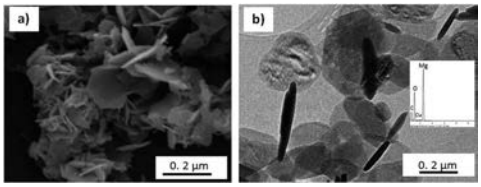

Fig. 2 (a) Low magnification SEM micrograph and (b) TEM micrograph of the synthesized $Mg(OH)_2$ nanoparticles. Inset shows the EDX spectrum of the nanoparticles.

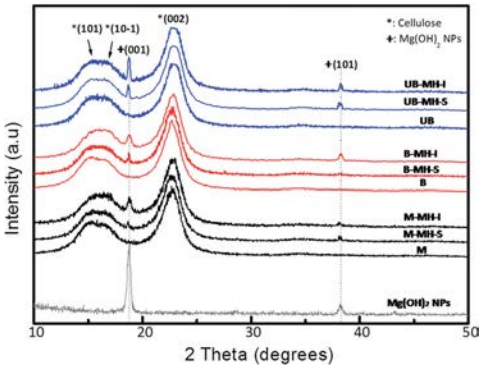

Fig. 3 XRD patterns of $Mg(OH)_2$ nanoparticles and $Mg(OH)_2$ modified cellulose sheets. The sheets were prepared from unbleached (UB), bleached (B) and mixture of the UB and B fibers (M).

prepared sample obtained by a hydrothermal method. This XRD pattern exhibited the typical diffraction peaks which were assigned to (001), (100) and (101) planes of the structure of $Mg(OH)_2$ (Joint Committee on Powder Diffraction Standards File (JCPDS) no. 44-1482, space group $P\bar{3}m1$ with unit cell parameters $a = 3.144$ Å and $c = 4.777$ Å). No additional XRD peaks arising from impurities were detected.

Based on these results, the obtained magnesium hydroxide nanoparticles were suitable for their application on cellulose fibers.

4.2. Cellulose structure and crystallinity index by X-ray diffraction (XRD)

X-ray diffraction (XRD) analysis was performed to study the crystalline structure and crystallinity of the cellulose samples and to determine the influence of the incorporation of $Mg(OH)_2$ on the cellulose structure. The X-ray diffraction patterns of the untreated and treated cellulose samples are shown in Fig. 3. All the cellulose samples exhibited the characteristic diffraction peaks of cellulose-I structure, a primary (002) crystallographic plane and a secondary overlapped (101) and (10−1) peak.[19,20] This is particularly important in the case of the cellulose sheets treated with hydroxide nanoparticles. While cellulose II crystals show no overall polarity due to the antiparallel arrangement of the chains, the cellulose I crystals exhibit high polarity (Samayam *et al.* 2011).[21] The pronounced polarity of these crystal domains may improve the interaction of the fibers with magnesium nanoparticles. In the treated cellulose samples, a few additional peaks corresponding to $Mg(OH)_2$ nanoparticles can also be noticed, confirming the successful coating of the fibers. The crystallite size of magnesium hydroxide nanoparticles on the cellulose composites calculated by Scherrer formula was 45 ± 3 nm. In addition, there was no significant difference in the crystalline structure of brucite after attachment to microfibrillated cellulose.

The crystallinity index of cellulose (CrI) was determined from XRD data by using the Segal method. The crystallinity index of 74% of unbleached cellulose fibers (UB) is lower than that of the bleached (B) fibers (CrI = 81%). The refining process induces an increase in crystallinity, which is also well documented in the literature.[22,23]

4.3. Surface morphology of cellulose fibers by scanning electron microscopy (SEM)

Morphological properties of as prepared cellulose sheets. Fig. 4 shows SEM micrographs of the UB-, B- and M-fiber sheets before and after treatment with $Mg(OH)_2$ nanoparticles. Fig. 4a, d and g depict the surface morphology of untreated sheets. Depending on the initial physical treatment, there is change in the morphology of the fibers. It is widely known that pulp refining (beating) can affect the properties of cellulose fibers through a variety of simultaneous.[1,2] The main effects of the refinement procedure are fibrillation (external and internal fibrillation), fines formation, fiber shortening and straightening.[24,25] According to Kang and Paulapuro,[26] the refining in a Valley beater increases simultaneously the internal and external fibrillation and facilitates the generation of fines. As can be seen in Fig. 4a, the UB fibers have well-preserved surfaces with no apparent fibrillation and no voids between fibers. Refined B-fibers (Fig. 4g) showed the increased fibrillation and fines generation on the cellulose surface with the formation of a gel like layer. The observed gelatinous layers could be produced during the fibrillation process by the dissolution of some hydrophilic compounds from the cell wall.[27] Mou *et al.*,[28] who studied the influence of low consistency refining on the morphology and the surface chemistry of pine pulp fibers, also showed the presence of a film-like formation that connect the fibers. They suggested that the film was formed out of the extracellular material as well as fine cellulosic fibrils. Furthermore, it can be seen that the refining produced the flattening of the fibers (Fig. 4b), which might be the result of the collapse of the fiber lumen during refining.[28,29] The fibrillation and generated fines as well as the gelatinous layers improved the interaction of cellulose fibers and reduce the number of voids between fibers after the sheet formation. This is especially apparent in the SEM micrograph of the sheet made of mixed fibers (Fig. 4c), which exhibit a high surface smoothness. An increase in smoothness of the sheets could be the consequence of the interaction of the lignin and hemicellulose cell wall residuals from the unbleached pulp with bleached cellulose fibers. This is in agreement with recent results of Ferrer *et al.*[30] who observed improved compaction of unbleached cellulose sheets during pressing and drying if the residual cell wall components were present. An improved interaction between UB- and B-fibers suggested by SEM may also have an effect on the mechanical properties of the M-sheets, which will be discussed further below.

The treatment of the cellulose sheets with $Mg(OH)_2$ nanoparticles. The SEM images of the cellulose sheets modified with nanostructured $Mg(OH)_2$ particles are shown in (Fig. 4d–i). The SEM analyses suggest that the attachment and dispersion of the

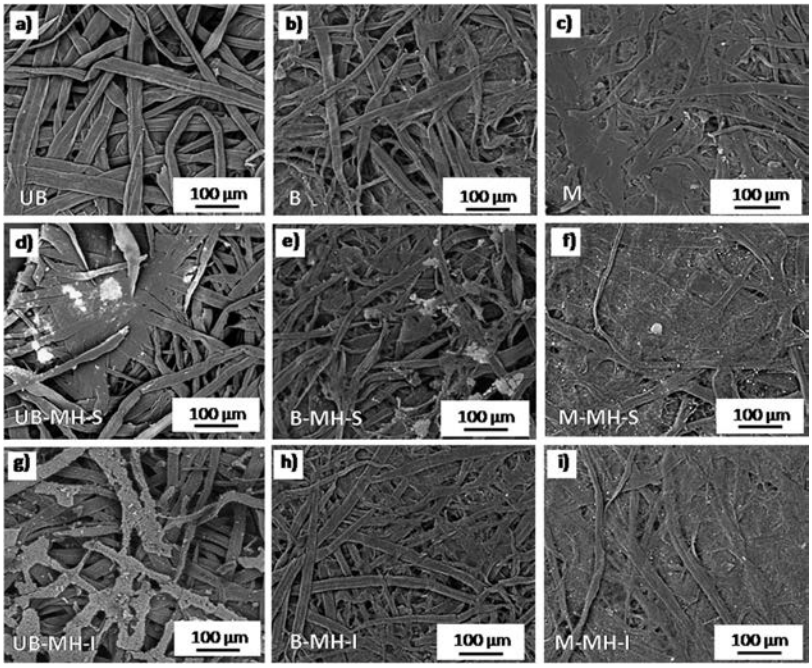

Fig. 4 SEM micrographs of UB, B and M cellulose sheets before and after modification with $Mg(OH)_2$ nanoparticles. First row: as prepared (a) UB, (b) B and (c) M sheets. The second row (d–f) and the third row (g–i) show SEM micrographs of $Mg(OH)_2$ modified UB, B and M samples prepared by spraying and immersion, respectively.

nanoparticles strongly depends on the refinement of the fibers. It can be seen in Fig. 4b and c that the particles tend to agglomerate on the surface of UB (unrefined) sample regardless of the application method used (spraying or immersion). In contrast, in the B and M samples the particles are more uniformly dispersed throughout the sample (Fig. 4e, f, h and i). As mentioned above, the refinement treatment induces pronounced fibrillation and fines generation, which consequently results in the appearance of an increased number of exposed OH groups in the samples. Since the OH groups are more accessible to interact with $Mg(OH)_2$ particles and the agglomeration will be reduced. It should also be noticed that the nanoparticles better penetrate in the sheets during the immersion process, which is in agreement with the literature results.[31] However; the degree of agglomeration is more dependent on the morphology of the fibers used for the preparation of the sheets. This is well-illustrated in Fig. 5, where we presented the higher resolution SEM micrographs of the sheets prepared by immersion into the $Mg(OH)_2$ nanoparticle solution (UB-MH-I, B-MH-I and M-MH-I samples). Again, better dispersion of the nanoparticles was noticed in the B-MH-I and M-MH-I sheets. For the successful preservation of the documentary heritage, an optimal penetration of the brucite nanoparticles into the sample is necessary and the observed effect should be taken into account.

4.4. Smoothness

Surface smoothness is one of the most important paper properties when it comes to printing application. The smoothness of a paper is affected by the raw material selection and its treatment as well as coating and finishing processes. The smoothness of the UB-, B- and M-sheets was tested before and after treatment with magnesium hydroxide nanoparticles. The obtained results are illustrated in Fig. 6. It was found that untreated B sheets have slightly lower smoothness than that of the UB sheets, 370 mL min^{-1} *versus* 466 mL min^{-1}, respectively. On the other hand, the smoothness of the sheet increases up to 780 mL min^{-1} if the mixture of the UB and B fibers was used in their fabrication. Obviously, the fibers of different morphologies pack better into the cellulose web and form more compact film. This is in agreement with SEM observations presented above (Fig. 4c). The modification with $Mg(OH)_2$ particles induce an increase in smoothness in all three types of the cellulose sheets. The nanoparticles probably improve the interaction between the adjacent fibers, which reduces the number of voids

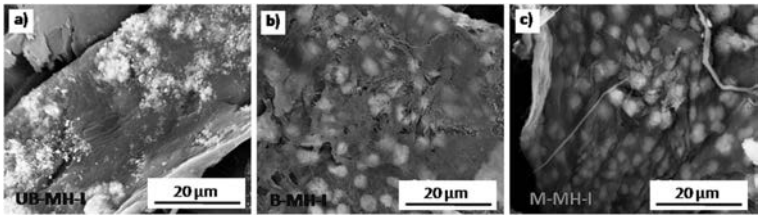

Fig. 5 SEM micrographs of (a) UB-MH-I, (b) B-MH-I and (c) M-MH-I samples at higher magnification.

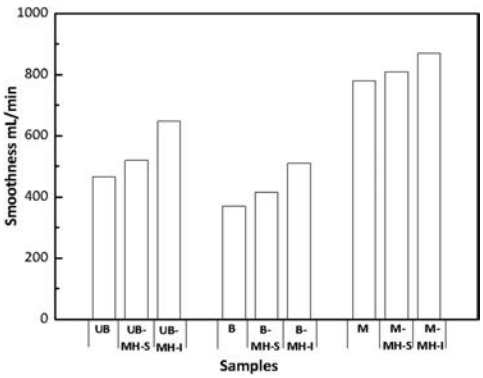

Fig. 6 Smoothness values of as prepared and $Mg(OH)_2$-modified fiber sheets.

and consequently improve the smoothness. We observed similar effect in our recent paper,[16] where ZnO nanoparticles were used for the fabrication of the papers for the antibody immobilization. Finally, the fact that the immersion process resulted with better penetration of the nanoparticles within the sheets is also reflected in smoothness tests. All three samples prepared by the immersion procedure (UB-MH-I, B-MH-I and M-MH-I), exhibited higher smoothness than their counterparts of the same fiber textures.

4.5. The mechanical properties

The results of the tensile test of the unmodified and $Mg(OH)_2$ nanoparticles modified sheets are shown in Table 2. The tensile index values of the as prepared sheets (UB, B and M) show the well-known that the fiber pre-treatment by beating strongly affects the final properties of the sheets. The control UB sample, has tensile index of 11.7 N mg^{-1}, which is significantly lower than that of B sample of 59.7 N mg^{-1}. The control M sheet has the highest tensile index of 70.1 N mg^{-1}, which again justifies our approach of using the mixture of refined and non-refined fibers in order to improve the properties of the paper sheets. The tensile index values of the sheets were not changed significantly after treatment with $Mg(OH)_2$ nanoparticles.

Table 2 Tensile indices of unmodified and $Mg(OH)_2$ modified fiber sheets after accelerated ageing

Sample	Tensile index (N mg^{-1})
UB	11.7
UB-aged	10.5
UB-MH-S-aged	11.0
UB-MH-I-aged	9.0
B	59.7
B-aged	56.5
B-MH-S-aged	58.0
B-MH-I-aged	57.2
M	70.1
M-aged	67.0
M-MH-S-aged	68.7
M-MH-I-aged	69.5

Although the nanoparticles improve the smoothness of the sheets, they do not affect significantly their strength. Finally, the mechanical tests were performed also on the untreated and treated samples subjected to artificial ageing. As the results in Table 2 show, the observed changes after the ageing were within the experimental error.

4.6. pH variation

Fig. 7 shows the variation of the pH of the cold water extracts after immersion of the cellulose sheets for one hour. The pH tests were performed on the unaged sheets and the sheets subjected to artificial aging. As expected, after the incorporation of the magnesium hydroxide nanoparticles in cellulose sheets, all the samples experienced an increase in their pH (Fig. 7). The untreated paper UB-, B- and M-sheets showed pH around 7, while the pHs of the UB-MH-I, B-MH-I and M-MH-I sample were in the range from 8 to 8.5. These values are close to the optimal pH value for paper protection of ~8.5 established in the literature.[32] It should be noted that it is very important to keep the pH within the proposed limits, especially when it comes to the preservation of the documentary heritage. At higher pH (around 10), it was found that the cellulose is susceptible to alkaline depolimerization.[33] Concerning the aged samples, slightly lower pH values are observed with respect to that of the initial sheets. Nevertheless, the observed changes were less than 5% proving the stability of the treated sheets on the possible effects of environmental stresses.

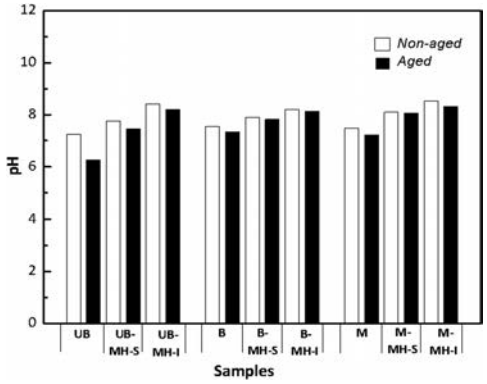

Fig. 7 The variation of the pH of the cold water extracts before and after ageing.

5. Conclusions

In this study, brucite magnesium hydroxide nanoparticles synthesized by the hydrothermal method were used for the treatment of the pine cellulose fiber sheets with different refining degree. The sheets were fabricated from bleached (B) and refined unbleached (UB) fibers as well as their 50%/50% mixture (M). They are treated with two main methods used for modification of the paper surface with inorganic dispersions: spraying and immersion. The structural and morphological analyses showed that the nanoparticles were successfully deposited onto sheets. The morphology of the sheets and the dispersion of the nanoparticles onto them strongly depended on the refinement of the fibers. The SEM analysis showed that the refined cellulose fibers (B type) exhibit pronounced fibrillation and the presence of fines together with the gel like layer throughout the cellulose web. The most compact sheet (M sheet) was obtained with the mixture of the fibers, probably due to stronger inter-fiber interactions. For this reason, the M sheets showed improved mechanical strength and smoothness with respect to the sheets prepared from the single fiber type. The treatment with $Mg(OH)_2$ nanoparticles did not affect significantly the mechanical properties but it did improved the smoothness of all three types of paper sheets studied here. The observed effects were slightly stronger when the immersion method for the deposition of the nanoparticles was used. Finally, comparing to the untreated sheets, the cellulose sheets treated with $Mg(OH)_2$ nanoparticles showed increased values of pH in the range from 8 to 8.5 which is the recommended value for the paper protection found in the literature. The pH values did not change significantly after the paper sheets were subjected to artificial aging. General conclusions are that the refining degree of cellulose played an important role in the treatment of the cellulose composites with magnesium hydroxide nanoparticles. In addition, treatment of the paper sheets with $Mg(OH)_2$ nanoparticles may be a good approach towards the successful protection of the paper documents against aging.

Acknowledgements

This study was supported by the Geomaterials 2 Programme (S2013/MIT_2914), the Innovation and Education Ministry (ref. MAT2013-47460-C5-5-P) and the Autonomous Region Program of Madrid, MULTIMAT-CHALLENGE (ref. S2013/MIT-2862). A. S.-F. would like to thank Dr Dušan K. Božanić, and Prof. Dr Vladimir Djoković for their trust and continuous encouragement.

References

1 D. C. Mcintosh, *Tappi*, 1967, **50**, 482–488.
2 X. Zeng, E. Retulainen, S. Heinemann and S. Fu, *Nord. Pulp Pap. Res. J.*, 2012, **27**, 335–342.
3 S. Gharehkhani, E. Sadeghinezhad, S. N. Kazi, H. Yarmand, A. Badarudin, M. R. Safaei and M. N. M. Zubir, *Carbohydr. Polym.*, 2015, **115**, 785–803.
4 F. Laoutid, L. Bonnaud, M. Alexandre, J. M. Lopez-Cuesta and P. H. Dubois, *Mater. Sci. Eng., R*, 2009, **23**, 100–125.
5 M. Ramin, H. Andres, A. Blüher, M. Reist and M. Wälchli, *J. Pap Conservat.*, 2009, **10**, 17–25.
6 R. Giorgi, L. Dei, M. Ceccato, C. Schettino and P. Baglioni, *Langmuir*, 2002, **18**, 8198–8203.
7 E. Stefanis and C. Panayiotou, *Restaurator*, 2007, **28**, 185–200.
8 G. Poggi, R. Giorgi, N. Toccafondi, V. Katzur and P. Baglioni, *Langmuir*, 2010, **26**, 19084–19090.
9 H. Chen, C. Xu, Y. Liu and G. Zhao, *Electron. Mater. Lett.*, 2012, **8**, 529–533.
10 S. Utampanya, K. J. Klaubunde and J. R. Schlup, *Chem. Mater.*, 1991, **3**, 175–181.
11 X. Li, C. Ma, J. Zhao, Z. Li, S. Xu and Y. Liu, *Powder Technol.*, 2010, **198**, 292–297.
12 H. Wu, M. Shao, J. Gu and X. Wei, *Mater. Lett.*, 2004, **58**, 2166–2169.
13 Q. Wang, C. Li, M. Guo, L. Sun and C. Hu, *Mater. Res. Bull.*, 2014, **51**, 35–39.
14 Q. L. Wu, L. Xiang and Y. Jin, *Powder Technol.*, 2006, **165**, 100–104.
15 L. Csóka, D. K. Bozanic, V. Nagy, S. Dimitrijevic-Brankovic, A. S. Luyt, G. Grozdits and V. Djokovic, *Carbohydr. Polym.*, 2012, **90**, 1139–1146.
16 V. Khatri, K. Halász, L. V. Trandafilovic, S. Dimitrijevic-Brankovic, P. Mohanty, V. Djokovic and L. Csóka, *Carbohydr. Polym.*, 2014, **109**, 139–147.
17 A. Sierra-Fernandez, L. S. Gomez-Villalba, O. Milosevic, R. Fort and M. E. Rabanal, *Ceram. Int.*, 2014, **40**, 12285–12292.
18 L. Segal, J. J. Creely, A. E. Martin and C. M. Conrad, *Text. Res. J.*, 1959, **29**, 786–794.
19 S. Xiao, R. Gao, Y. Lu, J. Li and Q. Sun, *Carbohydr. Polym.*, 2015, **119**, 202–209.

20 P. Bazant, I. Kuritka, L. Munster and L. Kalina, *Cellulose*, 2015, **22**, 1275–1293.
21 I. P. Samayam, B. L. Hanson, P. Langan and C. A. Schall, *Biomacromolecules*, 2011, **12**, 3091–3098.
22 N. Liu, M. Qin, Y. Gao, Z. Li, Y. Fu and Q. Xu, *Bioresources*, 2012, **7**, 3367–3377.
23 K. E. Borchani, C. Carrot and M. Jaziri, *Cellulose*, 2015, **22**, 1577–1589.
24 R. R. Hartmann, in *Mechanical treatment of pulp fibers for property development*, Institute of Paper Chemistry, Lawrence University, Appleton, Wisconsin, 1984.
25 S. Gharehkhani, E. Sadeghinezhad, S. N. Kazi, H. Yarmand, A. Badarudin, M. R. Safaei and M. N. M. Zubir, *Carbohydr. Polym.*, 2015, **115**, 785–803.
26 T. Kang and H. Paulapuro, *Pulp Pap. Can.*, 2006, **107**, 51–54.
27 P. Fardim and N. Duran, *Colloids Surf., A*, 2003, **223**, 263–276.
28 H. Mou, E. Iamazaki, H. Zhan, E. Orblin and P. Fardim, *Bioresources*, 2013, **8**, 2325–2336.
29 H. Mou, B. Li, E. Heikkila, E. Iamazaki, H. Zhan and P. Fardim, *Bioresources*, 2013, **8**, 5995–6013.
30 A. Ferrer, E. Quintana, I. Filpponen, I. Solala, T. Vidal, A. Rodriguez, J. Laine and O. J. Rojas, *Cellulose*, 2012, **19**, 2179–2193.
31 A. Wójciak, *Restaurator*, 2015, **36**, 3–23.
32 S. Sequeira, C. Casanova and E. J. Cabrita, *J. Cult. Herit.*, 2006, **7**, 264–272.
33 C. J. Knill and J. F. Kennedy, *Carbohydr. Polym.*, 2003, **51**, 281–300.